Journal of Nuclear Materials 408 (2011) 194–200

Contents lists available at ScienceDirect

Journal of Nuclear Materials

journal homepage: www.elsevier.com/locate/jnucmat

# Effects of solute atoms on evolution of vacancy defects in electron-irradiated Fe–Cr-based alloys

A.P. Druzhkov *, A.L. Nikolaev

*Institute of Metal Physics, Ural Branch RAS, 18 Kovalevskaya St., 620041 Ekaterinburg, Russia*

ARTICLE INFO

*Article history:*
Received 2 July 2010
Accepted 18 November 2010

ABSTRACT

The evolution of vacancy-type defects in Fe–Cr alloys (13–16 at.% Cr) undoped and doped with C, N, Au, or Sb and in conventional ferritic–martensitic steel (~13% Cr) has been investigated using positron annihilation spectroscopy under electron irradiation at room temperature and subsequent stepwise annealing. Small vacancy clusters are formed in the undoped Fe–16Cr alloy, which anneal out between 320 and 550 K. It is shown that oversized substitutional solute atoms (Sb, Au) in the Fe–Cr alloy interact with vacancies and form complexes, which are stable up to 600 and 420 K, respectively. It is found that the accumulation of vacancy defects considerably increases in the alloys and the steel with an enhanced content of interstitial impurities. It is shown that this effect is related to the formation of vacancy-carbon complexes. It is known that chromium in iron decreases the diffusion mobility of carbon. Therefore, the structure of vacancy-carbon complexes and the kinetics of their annealing in Fe–Cr alloys differ from those in the Fe–C system.



## 1. Introduction

Void swelling and radiation creep of nuclear materials, which are used for fuel cladding in breeder reactors, are controlled by migration of irradiation-induced defects. Low-activation ferritic/martensitic steels with 7–17 at.% Cr and smaller quantities of W, V, and Ta have been viewed recently as potentially superior alternatives to austenitic steels because of their higher swelling resistance and better thermal properties [1–3]. However, the physical basis of the swelling resistance in these materials has not been understood yet [4]. To solve this problem, the properties of irradiation-induced point defects need to be known first.

The recent studies [5] on resistivity recovery have pictured the evolution of radiation-induced defects in Fe–Cr model alloys upon annealing after low-temperature electron irradiation as follows. At temperatures of stage I (below 130 K), self-interstitial atoms (SIAs) in the form of mixed dumbbells are captured in configuration traps; that is, configurations consist of two chromium atoms, and the long-range migration of SIAs is suppressed up to 220 K. Stage III occurs near 205–210 K, and its position at the same concentration of vacancies almost coincides with that in pure iron [6]. Thus, the vacancy migration energies in Fe–Cr and pure iron are very close, while mobilities of SIAs are considerably different.

Unlike in the model alloys, the radiation damage of commercial steels is also affected by the interaction between radiation-induced defects and atoms of solute additives. Foreign interstitial atoms (FIAs) of carbon and nitrogen are the most frequent among the additives in commercial steels. Above their solubility limit, they are responsible for the formation of carbides and nitrides, which are very useful in improving the strength and hardness of steels [7]. Below their solubility limit, the presence of even a very little amount of these impurities (a few hundreds of appm) can have a drastic effect on the alloy properties, as they build strong interactions with point defects present in the irradiated steel [8]. The interaction of FIAs with vacancies in bcc Fe–Cr-based alloys is of special interest since in Fe vacancies and carbon form complexes stable up to 500 K [6].

These complexes in Fe are formed in two steps [9]. At the first step, vacancy-carbon atom (V-C) pairs are formed below 350 K. At the second step, near 350 K these pairs are decorated with solute carbon atoms, which become mobile before the V-C pairs dissociate. It is thought that just this decoration adds to the thermal stability of V-C complexes [9]. It is known that a chromium addition markedly retards the carbon and nitrogen migration in iron-based alloys [10]. Therefore, it is interesting to clarify whether FIAs have similar or different effects on behavior of the vacancy-type defects in Fe–Cr and iron.

This paper reports data on accumulation and subsequent annealing of radiation-induced defects in electron-irradiated Fe–Cr-based alloys (13–16% Cr) at room temperature (RT). Alloys of two types have been investigated. The first type is a model alloy of a sufficiently high purity, and the second type is alloys of technical purity (technical alloys) containing considerable amounts of FIAs and a conventional 13Cr–1Mo ferritic–martensitic steel

* Corresponding author. Tel.: +7 343 378 38 62; fax: +7 343 374 52 44.
*E-mail address:* druzhkov@imp.uran.ru (A.P. Druzhkov).

0022-3115/$ - see front matter © 2010 Elsevier B.V. All rights reserved.
doi:10.1016/j.jnucmat.2010.11.036

(EP-450 in Russian notation). Some data for the technical alloys have been published previously [11].

Defects were diagnosed using the positron annihilation spectroscopy (PAS), whose physical principles are described comprehensively in [12]. It is well known that positrons are a sensitive probe of vacancy-type defects, with sensitivity starting from the atomic size to large vacancy clusters and nanovoids [13], whereas they are insensitive to interstitial atoms and their small agglomerates.

However, the annealing kinetics of the vacancy-type defects may be affected not only by the interaction of vacancies with solute atoms, but also by rearrangements of the interstitial-type clusters formed simultaneously. One of the possible ways of detecting such rearrangements is to immobilize vacancies in a special alloy up to as high temperature as possible and to monitor the positron annihilation parameters in the temperature range, in which vacancies are immobile. Any changes in the parameters would indicate rearrangements of the interstitial-type clusters, which can affect annealing of the vacancy-type defects.

It is known that atoms of substitutional impurities such as Au and Sb form complexes with vacancies stable up to 450 K and 620 K, respectively, in iron [14]. Therefore, doping with these impurities can be considered as a way to provide monitoring the stability of the interstitial-type defects if the interaction between the impurity atoms and vacancies is similar to that in iron. In this connection, we have investigated additionally two model alloys doped with Au and Sb.

## 2. Characterization of the materials and methods

The preparation of the model Fe–16% Cr alloys is described in Ref. [15]. The technical alloys and the EP-450 (13Cr1MoNbV) conventional ferritic–martensitic steel were produced at Bardin Institute of Metallurgy (Moscow) from raw materials similar to those used for the model alloys.

After rolling, cutting and electrical polishing, the samples about $10 \times 10\ mm^2$ in size (~0.2 mm thick) were annealed under a $10^{-5}$ Pa vacuum according to the following regimes: (1) all alloys, at 1070 K (in ferritic area) for 4 h followed by air cooling; (2) steel, normalization treatment for 0.5 h at 1320 K and tempering for 1 h at 1020 K (N&T condition).

The chemical compositions of the alloys and the EP-450 steel are listed in Table 1, which also presents a brief designation of the used alloys. The concentrations of Au and Sb were controlled by weighing and were confirmed by the methods of Rutherford backscattering and X-ray microanalysis. The concentrations of FIAs were determined in our laboratory by means of nuclear reaction microanalysis. However, the concentration of FIAs is determined integrally – that is, in the solid solution and precipitates – by this method. It is known that the solubility of FIAs in Fe is low; for example, it is just 0.02% for N at 473 K [16]. To reduce the amount of dissolved nitrogen about 0.1 at.% Al was introduced into technical alloys (see Table 1). Similarly to chromium, aluminium has a strong affinity for nitrogen and forms AlN precipitates in the ferrite matrix [17]. In addition, raw carbonyl iron contains a large amount of adsorbed oxygen [15]; therefore, aluminium, which has not reacted with N, is oxidized. Thus, aluminium is not present in the solid solution. It may be expected that the larger fraction, at least, of nitrogen in the technical alloys precipitates as nitrides during the thermal treatment and subsequent cooling. As regards carbon, it looks rather probable that in the Fe–Cr–CI alloy all carbon is dissolved. Nothing can be said, *a prior*, on the state of carbon in Fe–Cr–CII alloy, whether all carbon is dissolved or some fraction has precipitated. A conventional TEM examination failed to reveal any nitrides or carbides in the alloys because of their small size and low density. Fortunately, the accumulation of vacancy defects under irradiation turned out a good indicator of the concentration of dissolved carbon in the steel and alloys (see Section 4.2). As follows from the results presented in the subsection, the concentration of the dissolved carbon in Fe–Cr–CII significantly exceeds that in Fe–Cr–CI.

The microstructure of the EP-450 steel is typical of tempered martensite [2]. Tempered lath martensite containing dislocations and $M_{23}C_6$ carbides is the primary structural feature. The average dislocation density is of $\sim 10^{14}\ m^{-2}$. The population of chromium-rich $M_{23}C_6$ carbides ~0.2 μm in size precipitate mostly along prior austenite grain boundaries and martensite lath boundaries.

The irradiation procedure at RT has been described elsewhere [18]. The maximum electron fluence was $2 \times 10^{23}\ m^{-2}$. According to the resistivity increments of the Fe–16Cr alloy after low-temperature irradiation [15] and the specific resistivity of the Frenkel pairs equal to 75 $\mu\Omega \times$ cm/at.% [5], a fluence of $1 \times 10^{22}\ m^{-2}$ corresponds to a damaging dose of $\sim 1.5 \times 10^{-4}$ dpa.

The irradiated samples were stepwise annealed (25–50 K per step with a holding time of 0.5–1 h, respectively) over the temperature range from 300 to 800 K (in a vacuum of $10^{-5}$ Pa above ~500 K).

Positron states in vacancy-type defects were diagnosed at RT by angular correlation of annihilation radiation (ACAR), which is one of the positron annihilation techniques [12]. The ACAR method was realized in a one-dimensional ACAR spectrometer providing a resolution of 1 mrad × 160 mrad. A $^{22}Na$ positron source of activity of 400 MBq was used. At least $6 \times 10^5$ coincidence counts were collected in each ACAR spectrum; the peak-to-background ratio was $\sim 10^3$. The ACAR spectra represented the dependence of the coincidence count rate on the angle $\theta$ ($\theta$ being the deviation of annihilation $\gamma$-quanta from anticollinearity). The angle $\theta = p_z/m_0c$, where $p_z$ is the transverse component of the momentum of an electron–positron pair, $m_0$ is the rest mass of an electron, and $c$ is the light velocity.

Changes in the shape of the ACAR spectra were characterized by the standard *S*-parameter [18]. The *S*-parameter is defined as the ratio of the low-momentum ($p_z \leqslant 3 \times 10^{-3}\ m_0c$) region to the total region, respectively. If positrons are trapped in vacancy-type defects, the *S*-parameter increases [12].

## 3. Results

### 3.1. Accumulation of vacancy defects

Fig. 1 presents dependences of the *S*-parameter on the electron fluence for the Fe–Cr, Fe–Cr–CI, and Fe–Cr–CII alloys and the EP-450 steel. The values of the *S*-parameter in the initial (before

**Table 1**
Amounts of alloying elements and impurities of the used alloys and steel (in at.%).

| Alloy designation | Cr | Sb | Au | Ni | Al | C | N | Mo | Nb | V | B | S | P |
|---|---|---|---|---|---|---|---|---|---|---|---|---|---|
| FeCr | 16.0 | – | – | 0.01 | – | – | 0.007 | – | – | – | – | – | – |
| Fe–Cr–Sb | 16.0 | 0.3 | – | 0.01 | – | – | 0.007 | – | – | – | – | – | – |
| Fe–Cr–Au | 16.0 | – | 0.13 | 0.01 | – | – | 0.007 | – | – | – | – | – | – |
| Fe–Cr–CI | 15.7 | – | – | 0.01 | 0.1 | 0.013 | 0.035 | – | – | – | – | – | – |
| Fe–Cr–CII | 13.4 | – | – | 0.01 | 0.1 | 0.05 | 0.08 | – | – | – | – | – | – |
| EP-450 | 13.9 | – | – | 0.38 | – | 0.7 | – | 1.0 | 0.36 | 0.21 | 0.02 | 0.04 | 0.04 |

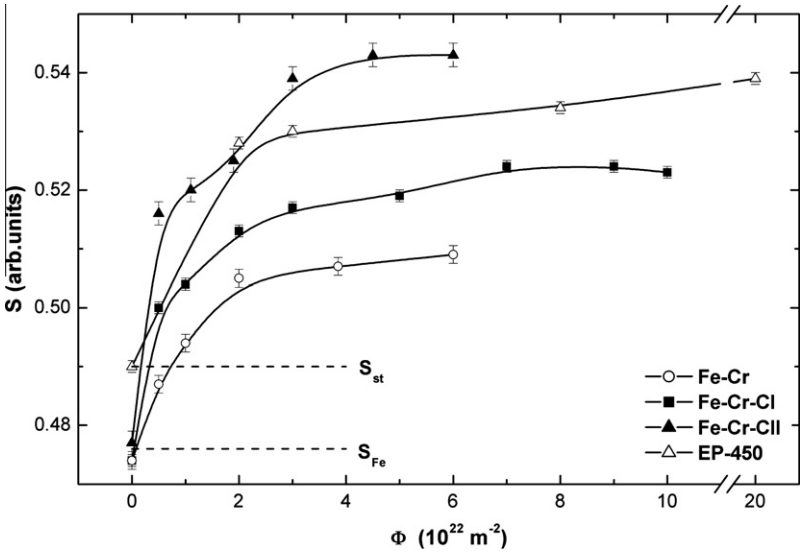


**Fig. 1.** Variation of the *S*-parameter as a function of the electron fluence for the Fe–Cr, Fe–Cr–CI, Fe–Cr–CII alloys and EP-450 steel irradiated at RT. The dashed lines indicate the levels of $S_{Fe}$, $S_{st}$ corresponding to the *S*-parameter values characteristic of positron annihilations from the bulk Fe and EP-450 steel (in N&T condition), respectively.

irradiation) state are the same for all the alloys and coincide with $S_{Fe} = 0.476 \pm 0.001$ for annealed pure Fe. Isolated atoms of the alloying elements and impurities in the solid solution and the possible presence of nitride and carbide precipitates in the matrix of the technical alloys do not influence the annihilation parameters. The positrons are not sensitive to the nitride (carbide) because its positron affinity is lower than that of the Fe matrix [19].

It should be noted that the initial (after N&T) value of the *S*-parameter for the steel, $S_{st} = 0.490 \pm 0.001$; is much larger than $S_{Fe}$. This is due to trapping of positrons at dislocations with density $\sim 10^{14}$ m$^{-2}$, which is much higher than the PAS sensitivity limit. An analogous microstructure with an enhanced dislocation density is also formed in other ferritic/martensitic steels after N&T [2].

Let us consider first the behavior of the *S*-parameter in the Fe–Cr model alloy. The dependence $S(\Phi)$ exhibits the following trend: (a) the *S*-parameter increases considerably as the fluence rises to $3.0 \times 10^{22}$ m$^{-2}$; (b) the *S*-parameter increases insignificantly at higher fluence values. Upon irradiation at RT, the migrating vacancies will both recombine with interstitial atoms and form small three-dimensional clusters. The increment of the *S*-parameter is due to trapping of positrons at small three-dimensional vacancy clusters (VCs).

The behavior of the dependence $S(\Phi)$ in the alloys doped with FIAs is similar to the behavior of the *S*-parameter in the model alloy. However, plateaus reached by the *S*-parameter are much higher, and this effect depends on the content of FIAs. The curve $S(\Phi)$ for the steel occupies an intermediate position between the curves for the Fe–CrI(II) alloys. Thus, the presence of a few hundreds of appm FIAs in the solid solution of the Fe–Cr–CI(II) alloys and the steel profoundly changes the accumulation of vacancy defects under irradiation.

The dependences $S(\Phi)$ for all the alloys and the steel are shaped as saturated curves; that is, the concentration of VCs and/or complexes is stabilized as the fluence increases. This is an indication that the clusters and the complexes are dominant sinks for SIAs and vacancies, which are mobile at RT [5,20].

### 3.2. Annealing of vacancy defects

#### 3.2.1. Fe–Cr, Fe–Cr–Sb, and Fe–Cr–Au alloys

Fig. 2 depicts the variation of the *S*-parameter on annealing of the Fe–Cr alloy irradiated to a fluence $5 \times 10^{21}$ m$^{-2}$ and $6 \times 10^{22}$ m$^{-2}$. The kinetics of recovery of the *S*-parameter depends on the fluence. Recovery in the low-fluence sample starts above 325 K and ends at 400 K. In the high-fluence sample, the main stage of recovery is observed at 400–550 K (see Fig. 2).

Fig. 3 presents dependences $S(T_{ann})$ for gold- and antimony-doped Fe–Cr alloys exposed to a fluence of $5 \times 10^{21}$ m$^{-2}$. The data on the Fe–Cr model alloy are given for comparison. As can be seen from Fig. 3, the dependences $S(T_{ann})$ for the model and the doped alloys are profoundly different. The increments of the *S*-parameter in the gold- and antimony-doped alloys upon irradiation are considerably larger if compared to those in Fe–Cr. The recovery of the *S*-parameter to its initial (before irradiation) value is shifted by 250 K or 400 K towards high temperatures in the cases of Au and Sb, respectively.

#### 3.2.2. Fe–Cr–CI and Fe–Cr–CII alloys and EP-450 steel

Fig. 4 shows the recovery of the *S*-parameter on annealing of Fe–Cr–CI, Fe–Cr–CII, and the steel irradiated to a fluence $2 \times 10^{22}$ m$^{-2}$. The increments of the *S*-parameter in the Fe–Cr–CII alloy and the steel are much larger than those in the Fe–Cr–CI alloy after irradiation. The stage of the *S*-parameter recovery is observed in the two alloys at temperatures of 325–400 K, with the recovery amplitude being higher in the Fe–Cr–CII alloy. The *S*-parameter is recovered continuously in the steel above 325 K, up to $S_{st}$ at ~600 K. When the Fe–Cr–CII alloy is annealed above 400 K, the *S*-parameter decreases continuously to its initial values at 600–620 K. In the Fe–Cr–CI alloy the *S*-parameter has two recovery stages at 400–450 K and 470–620 K in this temperature range.

Fig. 5 presents the dependences $S(T_{ann})$ for the Fe–Cr–CI(CII) alloys and the steel irradiated to fluencies $6 \times 10^{22}$–$2 \times 10^{23}$ m$^{-2}$. The dependence $S(T_{ann})$ for the Fe–Cr model alloy is given for comparison. It should be noted that the low-temperature stage (around 350 K) of the recovery is almost completely suppressed in the Fe–Cr–CI alloy. The main stage of recovery of the *S*-parameter is observed in the temperature range of (400–600 K), as in the model alloy. In the alloy with a high concentration of FIAs (Fe–Cr–CII) the values of the *S*-parameter are recovered continuously from 350 K to 600 K in one stage, similarly to their recovery after irradiation to a fluence $2 \times 10^{22}$ m$^{-2}$ (see Fig. 4). In the steel, the *S*-parameter also decreases continuously above 350 K and reaches $S_{st}$ at ~600 K.

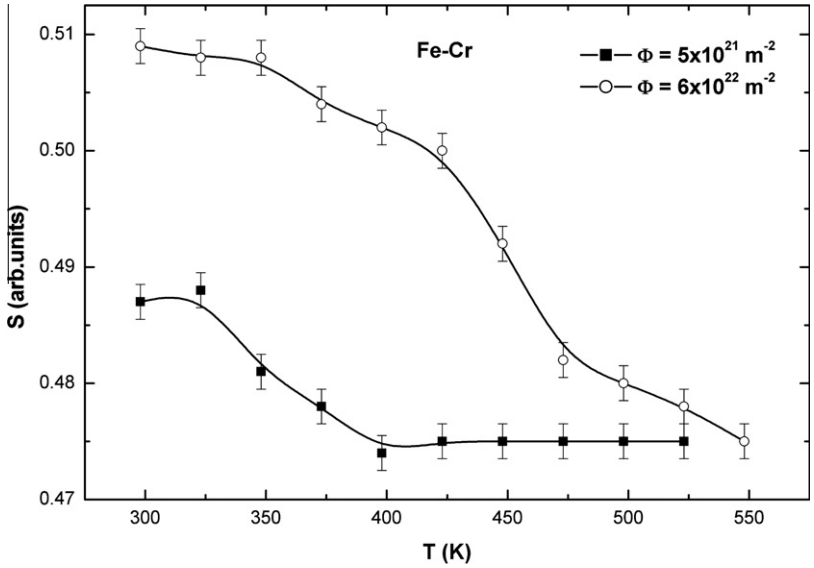


**Fig. 2.** Evolution of the *S*-parameter as a function of the annealing temperature in RT electron-irradiated Fe–Cr alloy with the lower and higher fluencies.

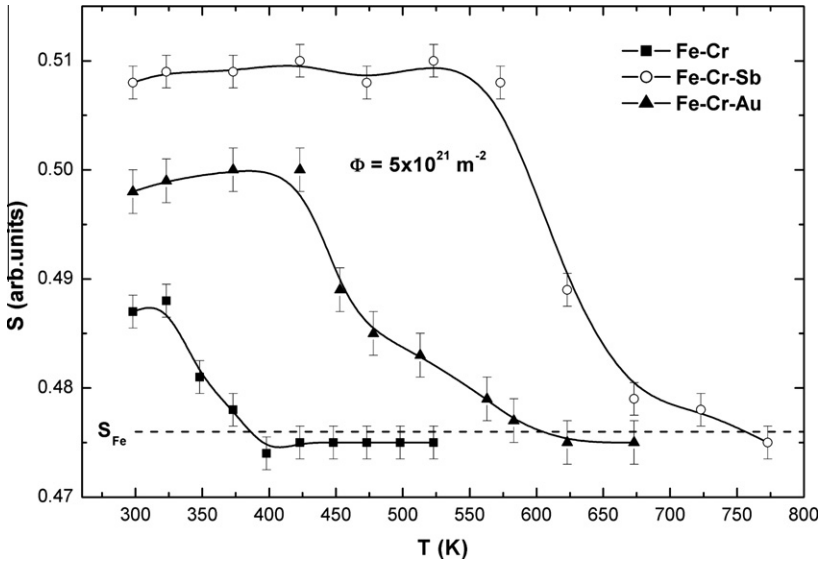


**Fig. 3.** Recovery of the *S*-parameter in electron-irradiated Fe–Cr, Fe–Cr–Au and Fe–Cr–Sb alloys at RT and $5 \times 10^{21}$ m$^{-2}$ fluence. The dashed line indicates the level of $S_{Fe}$ corresponding to the *S*-parameter value characteristic of positron annihilation from the bulk Fe.

## 4. Discussion

The results described in Section 3 show that interstitial and substitutional solute atoms may have a considerable effect on the accumulation and annealing of vacancy defects in the ferritic alloys. Let us discuss the specific features of the interaction between substitutional (Au and Sb) or interstitial (C and N) impurities and vacancies in Fe–Cr alloys as compared to those in Fe. Besides the mentioned impurities, our alloys contain also Al (Fe–Cr–Cl(II)) and Ni (all alloys). It has been mentioned above that Al is precipitated as AlN. As concerning Ni, we demonstrate below (Section 4.2.1) that it has no marked effect on accumulation of defects.

### 4.1. Effects of substitutional alloying elements

It is known [14] that oversized impurity atoms of Au and Sb strongly interact with vacancies in iron. The complexes formed are stable up to 450 K and 600 K, respectively.

An analogous situation is observed in the doped Fe–Cr alloys. The increment of the *S*-parameter is larger in the Fe–Cr–Sb alloy as compared to that of Fe–Cr after irradiation to $5 \times 10^{21}$ m$^{-2}$. It may be thought that doping with antimony has a result that most of the mobile vacancies, which are generated during irradiation at RT, form stable complexes with immobile Sb atoms. The values of the *S*-parameter are constant up to 600 K in the Fe–Cr–Sb alloy. That is, at temperatures below 600 K the complexes of vacancies and antimony atoms are stable. A rearrangement of the interstitial clusters, which can influence the kinetics of annealing of vacancy-type defects, is not observed either. The complexes dissociate above 600 K, and annealing of vacancy defects ends at 770 K.

The increment of *S*-parameter is smaller in the Fe–Cr–Au alloy than that in Fe–Cr–Sb after irradiation (see Fig. 3). This fact can be explained by a lower concentration of gold as compared to that of antimony. However, the dependence $S(T_{ann})$ in the Fe–Cr–Au alloy exhibits a similar behavior. The values of the *S*-parameter stay nearly unvaried up to 430 K. A decrease in the *S*-parameter, which

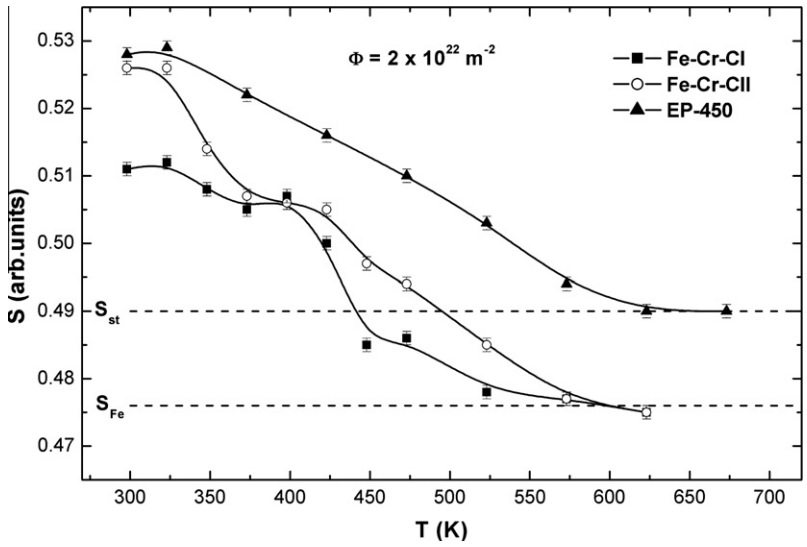


**Fig. 4.** Evolution of the *S*-parameter as a function of the stepwise annealing temperature in electron-irradiated Fe–Cr–Cl(II) alloys and steel at RT and $2 \times 10^{22}$ m$^{-2}$ fluence. The dashed lines indicate the levels of $S_{Fe}$, $S_{st}$ corresponding to the *S*-parameter values characteristic of positron annihilations from the bulk Fe and EP-450 steel (in N&T condition), respectively.

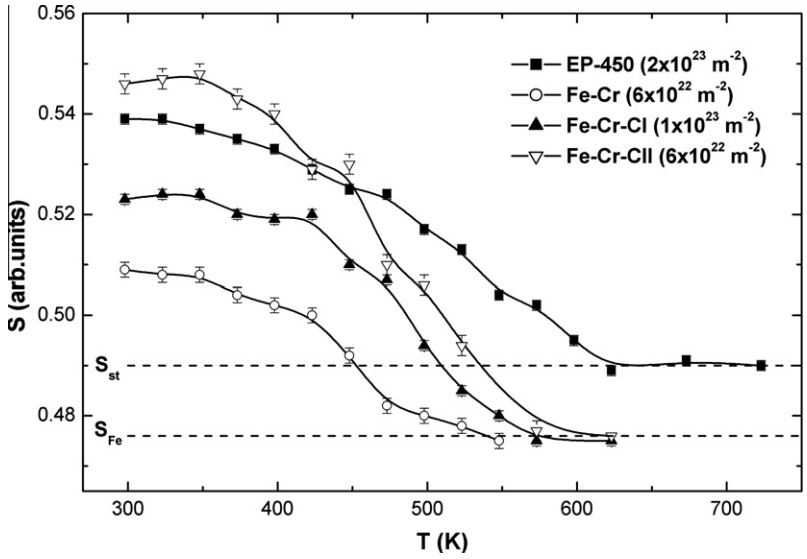


**Fig. 5.** Evolution of the *S*-parameter as a function of the stepwise annealing temperature in electron-irradiated Fe–Cr, Fe–Cr–Cl(II) alloys and steel at RT with different fluencies. The dashed lines indicate the levels of $S_{Fe}$, $S_{st}$ corresponding to the *S*-parameter values characteristic of positron annihilations from the bulk Fe and EP-450 steel (in N&T condition), respectively.

is caused by dissociation of the complexes, begins at annealing temperatures above 430 K, i.e., approximately at the same temperatures as in the Fe–Au system [14]. Annealing of the vacancy-type defects ends at 620 K.

It can be inferred that the energy characteristics of the interaction between substitutional alloying elements (Au and Sb) and vacancies in the Fe–Cr alloy are similar to those in pure Fe. On the other hand, as in iron, the structure of the interstitial-type defects does not exhibit changes leading to their recombination with vacancies, at least to 600 K.

### 4.2. Effects of interstitial impurities

#### 4.2.1. The role of nitrogen

Experimental data on the interaction of vacancies with nitrogen atoms are not available in Fe and Fe–Cr. Ab initio calculations of the interaction between FIAs and vacancies in iron obtain large values of the binding energy for "vacancy-nitrogen atom" (V-N) pairs, 0.71 eV [8] and 0.86 eV [21]. The carbon-free Fe–Cr model alloy contains ~70 at. ppm N (see Table 1). At a binding energy of 0.71–0.86 eV a V-N pair should be thermally stable near RT, and, therefore, vacancies in the Fe–Cr alloy should accumulate predominantly in the form of such pairs. In this case, the recovery curve of the *S*-parameter should be similar to the recovery curves for the Au- and Sb-doped alloys, in which the onset of the *S*-parameter drop corresponds to the beginning of dissociation of the vacancy-impurity pairs (see Fig. 3). According to [21], the energy of dissociation of V-N pairs in Fe is ~1.40 eV; that is, nitrogen should drastically decrease the mobility of vacancies (up to ~500 K). It is seen from Fig. 2 however that the recovery of the *S*-parameter in Fe–Cr irradiated to $5 \times 10^{21}$ m$^{-2}$ begins already at 320 K. This observation may be easily understood as an indication of instability of V-N pairs near RT. If V-N pairs are actually unstable, vacancies are expected to accumulate as VCs. An increased damage

should lead to a larger multiplicity and higher thermal stability of VCs and, correspondingly, to a shift of the *S*-parameter recovery towards higher temperatures. Namely, this feature is observed in the high-fluence Fe–Cr sample (Fig. 2).

Thus, the data on the recovery of the *S*-parameter in the Fe–Cr alloy evidence on a weak thermal stability of V-N pairs. This reasoning is in agreement with the recent data on the residual resistivity recovery of the Fe–4Cr alloy contained the close concentration of nitrogen [22]. According to [22], dissociation of V-N pairs takes place at 240–290 K. Thus, the calculations indicating a strong V-N interaction in Fe [8,21] are not consistent with the experimental data observed in the ferritic alloys. A weak V-N interaction also manifests itself in the kinetics of accumulation of vacancy defects at RT. The increment of *S*-parameter in the model Fe–Cr is the lowest as compared to the increments of technical Fe–Cr–CI(II) alloys contained carbon.

The same reasoning if applied in relation to the residual Ni gives evidence on a weak attraction between atoms of Ni and vacancies. This finding looks similar to that in the case of Fe, where V-Ni complexes disappear above 240 K [23].

*4.2.2. The role of carbon*

The interaction of carbon atoms with vacancies in Fe–C solid solutions has been studied well by both experimental [6] and calculation [9] methods. It was shown that at annealing temperatures above stage III (the stage, at which monovacancies become mobile, ~220 K for Fe [6]) migrating vacancies and carbon atoms form immobile V-C complexes. The binding energy of these complexes is 0.4–0.5 eV (see [9] and references therein).

The properties of V-C complexes in Fe have been successfully studied by PAS, specifically positron lifetime measurements [6,24]. A remarkable fact is strong positron trapping into the V-C pairs, which are formed in electron-irradiated Fe–C at annealing above the III stage temperature. As a result of the strong positron trapping into pairs, it argue [25] that the carbon atom is located off the center of the vacancy, e.g., the pairs do not recombine into a substitutional carbon atom, as there would then be no positron trapping. Such a structure of the pair is consistent with the calculations of Tapasa et al. [9], who reported that the distance between a vacancy center and a C atom, 0.36, is in units of the lattice parameter.

It may be expected reasonably that, by analogy with the Fe–C system, the Fe–Cr–CI(CII) alloys and the steel can also accumulate vacancy defects in the form of highly asymmetric V-C pairs, which are efficient traps of positrons. This is attested to by the data on the accumulation of vacancy defects (see Section 3.1 and Fig. 1). Large increments of the *S*-parameter in the carbon-containing alloys and steel suggest that a mutual recombination of vacancies with self-interstitial atoms under irradiation is suppressed because the mobility of vacancies decreases due to their capture by C atoms. As the carbon concentration increases, the accumulation of V-C pairs grows.

Let us discuss now the results of annealing of vacancy defects in carbon-containing alloys after irradiation to a low fluence (see Fig. 4) when the formation of V-C pairs dominates because the carbon concentration is much higher than the concentration of vacancies. In the temperature range of 320–400 K a stage of the *S*-parameter recovery is observed in the alloys, and this stage is pronounced most in the Fe–Cr–CII alloy with a high carbon concentration. This stage is also observed in electron- [6] and neutron-irradiated [26] Fe–C. It is known [6] that carbon atoms are mobile in Fe already at ~350 K. As a result, V-C pairs are decorated with 1–2 carbon atoms, and complexes of the V-2C type, which are stable up to 500 K [9], are formed at this stage. The efficiency of positron trapping by these complexes is reduced [25], and, therefore, the annihilation parameters decrease sharply to their initial values upon annealing in the range of 350–400 K [6].

In the Fe–Cr–CI(II) alloys this recovery stage can be related only to dissociation of V-C pairs and not to their decoration because mobility of carbon in Fe–Cr is suppressed. Chromium atoms have greater affinity for carbon than iron [10]. As a result, the energy state of carbon atoms in different octahedral sites is nonequivalent. It depends on whether the C atom is surrounded by Fe atoms only, or one or two Cr atoms are present in its nearest neighbourhood. Thus, the C atom in Fe–Cr is bound stronger, and it should surmount a large energy barrier for migration. As a result, its diffusion mobility is significantly decreased. For example, in the Fe–16% Cr alloy carbon is mobile at temperature ~540 K [10], which is much higher than in Fe (~350 K). For this reason, the decoration of V-C pairs or VCs with carbon atoms is highly improbable in our alloys.

The stage at ~350 K, which is associated with dissociation of V-C pairs, was also revealed by the recovery of the resistivity in an electron-irradiated Fe–4% Cr alloy [22]. The binding energy of V-C pairs is evaluated as $E_b \approx 0.4$ eV if the vacancy migration energy in Fe–Cr alloys is taken of 0.55 eV [20].

As the fluence increases, the stage around 350 K is practically suppressed in the alloy with a low C concentration (Fe–Cr–CI), whereas this stage is retained in the Fe–Cr–CII alloy (see Fig. 5). We assume that the formation of vacancy clusters dominates in the Fe–Cr–CI alloy, as the fluence grows. Using the positron lifetime measurements, we indeed detected [11] small VCs (~3 vacancies in a cluster) with a number density $N_{cl} = 1.2 \times 10^{23}$ m$^{-3}$ in the Fe–Cr–CI alloy irradiated to a fluence of $6 \times 10^{22}$ m$^{-2}$. The vacancy clusters dissociated above 400 K. The behavior of the dependence $S(T_{ann})$ for the Fe–Cr–CI alloy correlates well with the data on the lifetime [11] and $S(T_{ann})$ for the Fe–Cr model alloy (see Fig. 5). Similarly to the model alloy, the stage of annealing is observed above 400 K, which is connected with dissociation of VCs. Thus, it can be concluded that in the Fe–Cr–CI alloy with a low carbon concentration (~130 at. ppm) vacancy defects accumulate under irradiation in the form of V-C pairs and vacancy clusters. The formation of VCs prevails as the fluence increases.

In contrast to the Fe–Cr–CI alloy, the formation of V-C pairs dominates irrespectively of the fluence in the Fe–Cr–CII alloy with a high carbon concentration (~500 at. ppm). The recovery stage around 350 K is connected with dissociation of V-C pairs, which is observed in this alloy after irradiation to both low (Fig. 4) and high (Fig. 5) fluencies. Released upon dissociation of V-C pairs vacancies form clusters. The superposition of different processes, which are related to a rearrangement of VCs above 400 K (coarsening, dissociation), leads to a monotonic decrease in the *S*-parameter values during annealing of the Fe–Cr–CII alloy.

The following point is remarkable. If annihilation of positrons from the free state is neglected, the *S*-parameter in the irradiated Fe–Cr–CII alloy will be a weighted average value of the parameter for V-C pairs ($S_p$) and VCs ($S_{cl}$):

$$S = F_p S_p + (1 - F_p) S_{cl} \quad (1)$$

where $F_p$ is the fraction of positrons annihilating in the pairs. Since $S_p < S_{cl}$ [12], a large increment of the *S*-parameter in the Fe–Cr–CII alloy can be ensured if the concentration of the pairs is at least one order of magnitude higher than the number density of VCs; that is, $F_p \approx 1$ (see Ref. [6]).

Vacancy defects accumulate less in the EP-450 steel than in the Fe–Cr–CII alloy (see Fig. 1). The stage around 350 K, which is related to the decomposition of V-C pairs, is observed in the steel, too (see Fig 4). If it is assumed that the increment of the *S*-parameter under irradiation is also due to accumulation of V-C pairs, one can conclude that the concentration of carbon in the solid solution of the EP-450 steel is lower than it is in the Fe–Cr–CII alloy. The evaluation with the "THERMOCALC" software [27] indeed showed that the equilibrium concentration of carbon in the solid solution of ferritic–martensitic steels after the N&T treatment is

50–130 at. ppm depending on the concentration of alloying carbide-forming (V, Nb) elements and N&T regimes. On the other hand, vacancy defects accumulate more in the steel than in the Fe–Cr–CI alloy (see Fig. 1). That is, if it is assumed that all carbon in the Fe–Cr–CI alloy is in the solid solution, then the carbon concentration of the solid solution steel should be higher than 130 at. ppm. It should be remembered however that complexes of vacancies with other alloying or impurity atoms can add to the accumulation in the steel.

## 5. Conclusions

PAS was employed to study vacancy defect evolution in Fe–Cr-based alloys. Model (Fe–Cr, Fe–Cr–Sb, Fe–Cr–Au) and technical Fe–Cr–CI(II) alloys and the EP-450 steel were electron-irradiated at RT and subsequently stepwise annealed. The main results are summarized as follows.

1. In the Fe–Cr alloy oversized substitutional alloying elements (Sb, Au) interact with vacancies and form V-Sb and V-Au complexes, which are stable up to 600 and 420 K, respectively. The behavior of these alloying elements in the ferritic alloy is analogous to their behavior in Fe.
2. The mobile vacancies, which are generated during irradiation at RT, form stable V-C pairs with immobile carbon atoms in the Fe–Cr–CI(II) alloys and the steel. As a result, the accumulation of vacancy defects under irradiation increases. This effect is enhanced with growing content of carbon in the solid solution.
3. Around 350 K the recovery stage is observed in the Fe–Cr–CI(II) alloys like in Fe–C system. However, in iron this stage is related to decoration of V-C pairs with mobile carbon atoms and formation of vacancy-multi-C atom complexes, which are stable up to 500 K [9]. In Fe–Cr alloys the mobility of carbon atoms is considerably suppressed as compared to that in Fe, and, therefore, this stage is associated with dissociation of V-C pairs. Released upon dissociation of the pairs vacancies form vacancy clusters, which are annealed out between 550 and 650 K. These results are important for understanding the fundamental vacancy-solute interaction and the mechanism of the radiation damage in ferritic–martensitic steels.

## Acknowledgements

We are thankful to Dr. D.A. Perminov for his assistance during preparation of the manuscript. This work was done within RAS Program (Project No. 01. 2. 006 13394), with partial support of Ural Branch RAS (Project No. 09-M-23-2004).

## References

[1] E. Daum, K. Ehrlich, M. Schirra (Eds.), Development of Ferritic/Martensitic Steels for Fusion Technology, FZKA-5848, 1997.
[2] A. Zeman, L. Debarberis, J. Kocik, V. Slugen, J. Nucl. Mater. 362 (2007) 259–267.
[3] G. Bonny, D. Terentyev, L. Malerba, Scripta Mater. 59 (2008) 1193–1196.
[4] Z. Yao, M. Hernandez-Mayoral, M.L. Jenkis, M.A. Kirk, Philos. Mag. 88 (2008) 2851–2880.
[5] A.L. Nikolaev, Philos. Mag. 87 (2007) 4847–4874.
[6] A. Vehanen, P. Hautojarvi, J. Johansson, J. Yli-Kauppila, P. Moser, Phys. Rev. B 25 (1982) 762–780.
[7] R.L. Klueh, ORNL/TM-2004/176.
[8] C. Domain, C.S. Becquart, J. Foct, Phys. Rev. B 69 (2004) 144112.
[9] K. Tapasa, A.V. Barashev, D.J. Bacon, Yu.N. Osetsky, Acta Mater. 55 (2007) 1–11.
[10] I.A. Tomilin, V.I. Sarrak, N.A. Gorokhova, S.O. Suvorova, L.L. Zhukov, Engl. Transl. Sov. Phys. Met Metallogr. 56 (3) (1983) 74–79.
[11] V.L. Arbuzov, A.P. Druzhkov, A.L. Nikolaev, S.M. Klotsman, Rad. Eff. 124 (1992) 409–415.
[12] R.W. Siegel, Ann. Rev. Mater. Sci. 10 (1980) 393–425.
[13] M. Eldrup, B.N. Singh, J. Nucl. Mater. 251 (1997) 132.
[14] P. Moser, C. Corbel, P. Lucasson, P. Hautojarvi, Mater. Sci. Forum 15–18 (1987) 925.
[15] A.L. Nikolaev, J. Phys.: Condens. Matter 11 (1999) 8633.
[16] E.H. De Marchie van Voorthuysen, B. Feddes, N.G. Chechenin, Phys. Status Solidi (a) 177 (2000) 127.
[17] A.R. Clauss, E. Bischoff, R.E. Schacherl, E.J. Mittemeijer, Philos. Mag. 89 (2009) 565–582.
[18] A.P. Druzhkov, D.A. Perminov, A.E. Davletshin, J. Nucl. Mater. 384 (2009) 56–60.
[19] G. Brauer, M.J. Puska, M. Sob, T. Korhonen, Nucl. Eng. Des. 158 (1995) 149.
[20] C. Dimitrov, A. Benkaddour, C. Corbel, P. Moser, Ann. Chim. Fr. 16 (1991) 319–324.
[21] T. Ohnuma, N. Soneda, M. Iwasawa, Acta Mater. 57 (2009) 5947–5955.
[22] A.L. Nikolaev, Philos. Mag. (2011), doi:10.1080/14786435.2010.534740.
[23] A. Moslang, E. Albert, E. Recknagel, A. Weidinger, P. Moser, Hyperfine Interact. 17–19 (1984) 255–260.
[24] Y. Nagai, K. Takadate, Z. Tang, H. Ohkubo, H. Sunaga, H. Takizawa, M. Hasegawa, Phys. Rev. B 67 (2003) 224202.
[25] M.J. Puska, R.M. Nieminen, J. Phys. F: Met. Phys. 12 (1982) L211–L216.
[26] M. Weller, J. Diehl, W. Triftshauser, Solid State Commun. 17 (1975) 1223.
[27] M.H. Mathon, Y. de Carlan, G. Geoffroy, X. Averty, A. Alamo, C.H. de Novion, J. Nucl. Mater. 312 (2003) 236–248.